Paul Wu*, Yindong Yang, Mansoor Barati and Alex McLean

Electromagnetic Levitation of Silicon and Silicon-Iron Alloy Droplets

Abstract: In this paper, the design of an electromagnetic levitation system and a technique for non-conductive silicon heating and conductive silicon levitation is described. The aim of the work is to describe the various parameters including coil design, applied power and specimen weight that govern the temperature of levitated silicon and silicon-iron alloy droplets.

Keywords: metallurgical grade silicon, solar grade silicon, photovoltaic industry, electromagnetic levitation

PACS® (2010). 81.05.-t

***Corresponding author: Paul Wu:** Department of Materials Science and Engineering, University of Toronto, Ontario M5S 3E4, Canada. E-mail: paul.wu@mail.utoronto.ca

Yindong Yang, Mansoor Barati, Alex McLean: Department of Materials Science and Engineering, University of Toronto, Ontario M5S 3E4, Canada

1 Introduction

In recent years, the world's photovoltaic (PV) industry has experienced rapid development and expansion, attracting considerable attention from different industrial sectors. However, a shortage of raw materials with high purity and low cost restricts major development of this clean energy industry. At present, expensive semiconductor grade silicon (SEG-Si) is used for the manufacture of cells to convert solar energy into electricity. This results in a high cost for photovoltaic electricity compared to electricity derived from conventional sources. Since the amount of SEG-Si scrap supply is limited, an innovative process for silicon production using relatively inexpensive metallurgical grade silicon (MG-Si) as a starting material could provide a more economical route for the manufacture of solar cells.

A number of research studies have been carried out to upgrade metallurgical grade silicon to solar grade silicon [1–6]. For example, acid leaching, slag refining, thermal plasma processing, controlled solidification and vacuum melting have all been investigated. While solidification refining is an effective way to remove most of the impurities and does not require chemical processing, phosphorus and boron are not removed by this approach. There is therefore considerable interest in developing new processes for dephosphorization of silicon, as well as the removal of boron, in order to provide material which could then be used for solar grade applications. A potential method for the removal of phosphorus is to apply reduced pressure.

Electromagnetic levitation is an ideal tool to study gas-metal interactions and related kinetics owing to inherent advantages such as inductive stirring and approximate spherical geometry of the levitated droplet with associated high specific surface area. In addition, unlike other processes which use containers, levitation refining avoids potential contamination of the molten silicon by container materials. The aim of this work is to develop an electromagnetic levitation facility that would be suitable for the investigation of the thermodynamic and kinetic factors that affect the removal of phosphorus from metallurgical grade silicon or ferrosilicon alloys.

In the following sections, details are provided concerning some fundamental considerations pertaining to electromagnetic levitation, construction of the levitation assembly, aspects related to coil design, alloy preparation, calibration of the temperature measurement system, and factors affecting the levitation and temperature control of silicon alloy droplets.

2 Principle of electromagnetic levitation

A conductor can be made to levitate by balancing the electromagnetic body force (Lorentz force) and the gravity force which can be described using the governing equation [7]:

$$J \times B = \rho g \tag{1}$$

where J is the eddy current induced by the alternating magnetic field B, ρ is the density of the levitated material and g is the gravitational constant. For a levitation (or

solenoid) coil, the B function can be obtained by solving the Biot-Savart equation [8]:

$$dB = \frac{\mu_m I}{4\pi} \frac{dl \times r}{r^3} \tag{2}$$

where μ_m is the magnetic permeability of the material, I is the coil current (power), r is the radial position, and dl is the length element along the current path. The direction of the field dB is normal to a plane containing dl.

The eddy current J flows in an electrically conductive media, in this case molten metal, and has two main contribution sources 1) current induced by an alternating magnetic field and 2) current induced by the motion of an electrically conductive fluid under a magnetic field which can be expressed mathematically as follows [7]:

$$J = \sigma\left[\left(-\frac{\partial A}{\partial t}\right) + (v \times B)\right] \tag{3}$$

where σ is the electrical conductivity of the molten metal, v is the flow velocity, and A is the vector potential of a magnetic flux, defined as $B = \nabla \times A$, $\nabla \cdot A = 0$.

Although a full solution of the system may not be trivial, it is still possible to relate the coil current (applied power) to the gravity force (sample mass) by solving the above equations while taking account of joule heating, and heat dissipation through radiation loss. A conventional solution [9] of the system can be found in the fundamental principle of electromagnetic casting which utilizes the following relation:

$$\rho g h = \frac{B^2}{2\mu_m} \tag{4}$$

The magnetic field inside a levitation coil can be approximated with a solenoid infinite in length. A simplified solution to the Biot-Savart equation is [9]:

$$B = \mu_0 \frac{N}{L} I \tag{5}$$

where μ_0 is the magnetic constant, N is the number of turns and L is the length of solenoid. This solution, however, implies that B is independent of the length and diameter of the solenoid; and is uniform over the cross-section of the solenoid. Upon combining the two equations, we obtain:

$$\rho g h = \frac{{\mu_0}^2}{2\mu_m}\left(\frac{N}{L}\right)^2 I^2 \tag{6}$$

This expression served as a useful tool in the initial development of the coil design used in the present work.

3 Construction of equipment

3.1 Design and construction of the electromagnetic levitation facility

A schematic representation of the electromagnetic levitation facility is shown in Figure 1. The equipment consists of a quartz tube, a levitation coil, an aluminum rotatable platform, a copper mold and a specimen charging rod. The quartz tube, 15 mm in outer diameter, 13 mm in inner diameter and 304 mm in length, is sealed at the upper end with o-rings and a quartz window to permit temperature measurement using a two-colour IR pyrometer. Due to potential heating of metallic components as a result of the alternating electromagnetic field, polycarbonate and polyvinylchloride were used for the making of various parts with the exception of the aluminum base plate. The o-ring sealed, rotatable aluminum platform was located at the lower end of the chamber. This platform was fitted

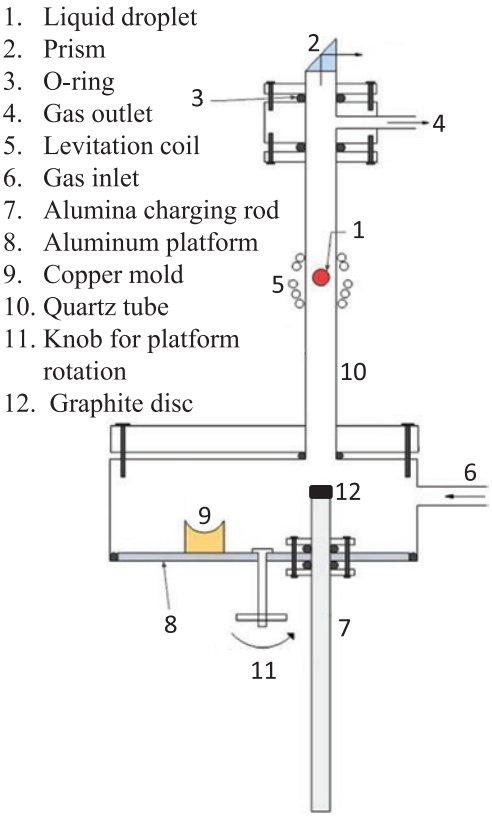

Fig. 1: Schematic diagram of the electromagnetic levitation assembly

with a copper mold for droplet quenching and an alumina charging rod for loading solid specimens into the electromagnetic field within the levitation coil. The rotating action of the platform allowed either the copper mold or the charging rod to be aligned directly below the levitation zone within the quartz tube. The water-cooled levitation coil was wound from copper tubing of 3.2 mm in outer diameter. After levitation, the liquid metal samples are quenched by dropping into the copper mold and subsequently analyzed.

3.2 Power supply and coil design

For any given experiment, the parameters that influence droplet temperature and droplet stability are the magnitude of the applied current, the coil geometry, the gas composition and flow rate, the specimen material and specimen mass. The power supply used in this investigation was a high frequency induction heating system by Ameritherm-Ambrell with a rated terminal output of 10 kW and a frequency range from 150 to 400 kHz. The magnitude of the applied current allows the manipulation of the droplet position within the levitation coil. There exists, however, a minimum working current that is required to support the droplet and this is influenced by the specimen material and mass, gas direction and flow rate as well as the coil design.

Droplet stability depends to a large extent on the coil design, which may be cylindrical or conical in shape with different coil angles. Levitation coils are generally derived empirically based on the design used by Harris and Jenkins [10]. Kermanpur et al. [11] have carried out detailed investigations in an attempt to provide a theoretical background for coil design by studying the effect of coil angle, number of horizontal turns, charge weight, and droplet vertical position, on lifting force and temperature profile within the droplet. A numerical model was developed to simulate the field generated by the coil using the finite element method. It was concluded that increase in coil angle (deviation from cylindrical geometry) will lead to a decrease in lifting force and in turn cause droplet temperature to increase as a result of the droplet location shifting to a lower position within the coil where the heating effect is stronger. As a design constraint, the oscillation frequency of the coil must match that of the power generator via mutual inductance. The coil's inductance, which varies with distance that separates each coil turn, may be altered to match the specified working range set by the generator. Generally, the coil's inductance decreases with increasing distance between the turns.

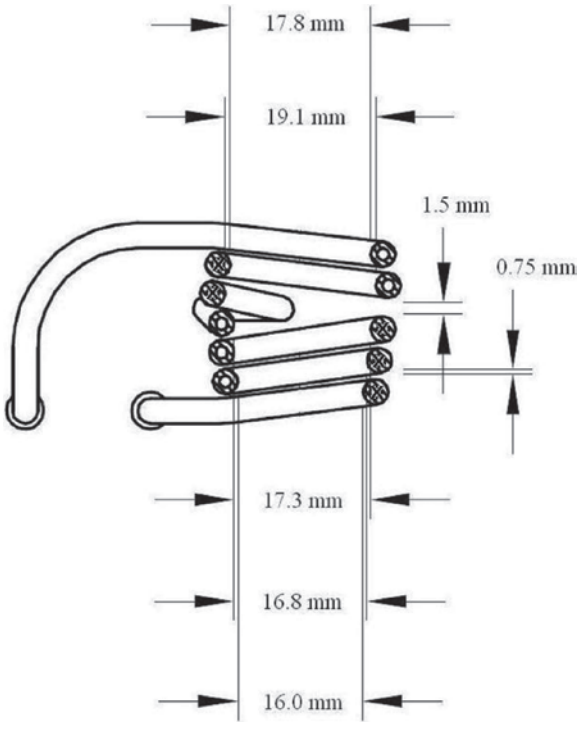

Fig. 2: Schematic diagram of the levitation coil

The design for the levitation coil used in this investigation is shown in Figure 2. After numerous tests, the selected coil consisted of a low-angle conical configuration that provides sufficient lift force, good droplet stability and appropriate droplet temperatures. The coil consists of two segments with the lower cone having three turns and the upper inverted cone having two reverse turns. The lower cone is responsible for providing the droplet with lifting force and heat while the upper inverted cone controls the vertical and lateral stability of the levitated droplet.

4 Experimental considerations

4.1 Master alloy preparation

Si-Fe alloys with different compositions were synthesized for experiments involving levitated droplets. In preparation of homogenized molten alloys, predetermined amounts of silicon of 6N purity were added to similarly pure iron ingots in a high purity alumina crucible. The crucible and its contents were heated in an induction unit as shown in Figure 3. Inside the chamber, an inert atmosphere was maintained by a constant flow of purified argon gas. Sufficient time was given to ensure complete homogenization of the molten alloy. Melt temperature was

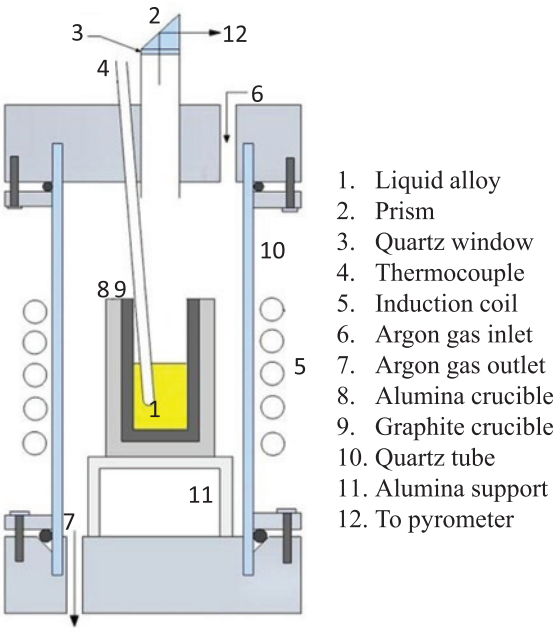

Fig. 3: Schematic diagram of the induction furnace system for preparation of silicon-iron alloys

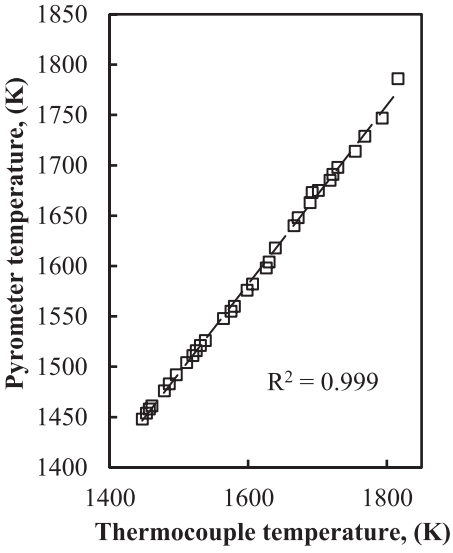

Fig. 4: Pyrometer calibration results obtained using the assembly shown in Figure 3

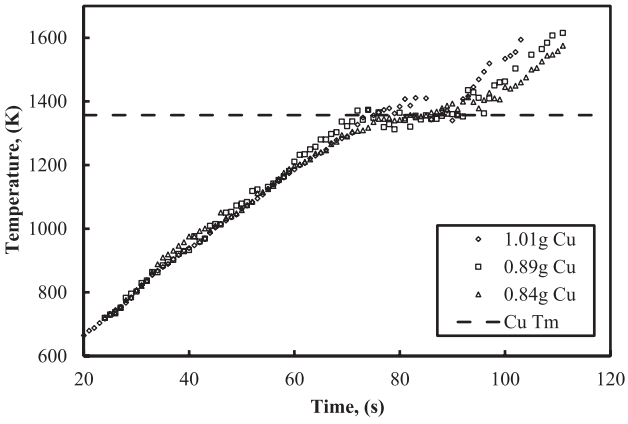

Fig. 5: Pyrometer calibration using copper droplets of different mass

monitored using both a thermocouple and a two-color optical pyrometer. Alloy samples were taken by suction through a quartz tube, thereby producing rod-shaped specimens with a diameter of 4 mm. These rods were then cut into small sections 0.6 to 1 gram in weight.

4.2 IR pyrometer calibration

In this study, temperature measurements were obtained using a Chino two-color pyrometer having an estimated uncertainty of ±15 degrees. The pyrometer was focused on the droplet in the levitation chamber or on the surface of the melt contained in the crucible within the induction furnace. An optical grade fused silica window (2 mm in thickness) and prism were used in order to minimize potential spectral loss during temperature measurements. Two calibration tests were carried out. For the first calibration, reference temperature measurements obtained with the thermocouple were used to calibrate the pyrometer readings using the furnace arrangement shown in Figure 3 with molten iron contained in an alumina crucible. The accuracy of the thermocouple was checked against the melting point of iron prior to calibration of the pyrometer. During the calibration tests a hydrogen-argon atmosphere was maintained within the induction unit to prevent oxidation of the molten iron. The results obtained in this way are shown in Figure 4. For the second set of experiments, the electromagnetic levitation facility was used to check the pyrometer calibration by measuring the melting point of copper droplets with different mass. The results are shown in Figure 5.

4.3 Levitation of silicon and silicon-iron alloy droplets

Since the resistivity of pure silicon is too high for samples to be electromagnetically levitated at temperatures below 1100 K, an additional pre-heating step is required. There are several preheating techniques reported in the literature associated with investigations of crystallization behavior and physical property measurements of highly undercooled silicon melts. Kuribayashi et al. [12–14] transmitted a CO_2 laser beam with wavelength of 10.6 μm onto

the silicon specimen to increase temperature high enough so that the droplet conductivity reaches the working range for levitation. For drop-shaft microgravity experiments [15, 16] an infrared heating device was implemented for preheating the metal specimen. Li et al. [17] suggested preheating be carried out in a resistance furnace positioned directly above the levitation coil. The work by Przyborowski et al. [18] has demonstrated the possibility of levitating single crystal silicon without preheating. It has been shown that B and Sb doped silicon displayed significantly lower resistivity than pure silicon and that levitation and subsequent melting was achieved.

In the present work, a silicon specimen was first placed on a high purity graphite disc located on the alumina charging rod as shown in Figure 1. The approach is similar to that by Li and Herlach [19] where a graphite heating element was encapsulated by an alumina shell. The graphite disc is then heated by induction as a result of the applied electromagnetic field. The resulting thermal energy is transferred from the graphite disc to the solid silicon by conduction. Decreased resistivity causes the solid specimen to respond to the applied field and begin to gain heat and ultimately levitate. The alumina charging rod is retracted as soon as a stable levitation condition is attained. In the case of silicon-iron specimens, preheating is also necessary but this can be achieved without utilizing the graphite disc. Iron within the silicon-iron alloy is responsible for providing inductive heating to the entire specimen. In the vicinity of 900 K, silicon-iron specimens respond to the applied field and begin to levitate. Photographs of a levitated silicon alloy droplet and as-quenched silicon sample are shown in Figure 6 and Figure 7, respectively.

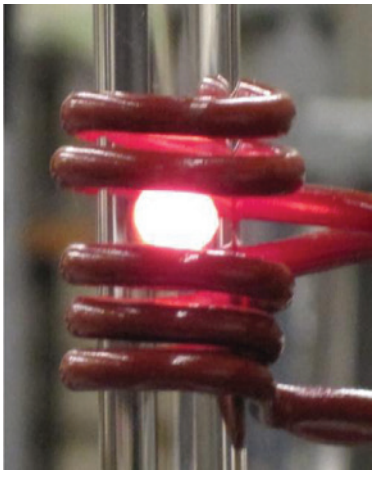

Fig. 6: Levitation of a silicon alloy droplet

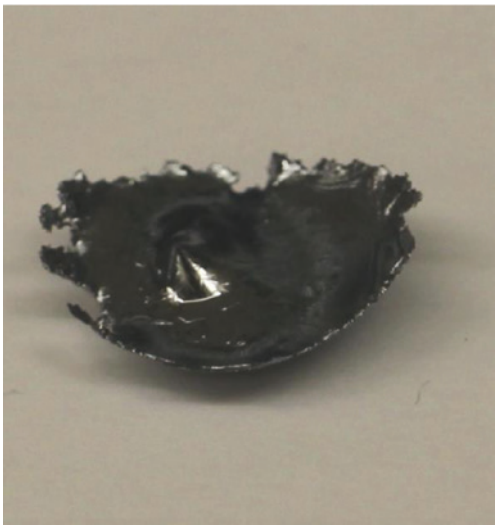

Fig. 7: Quenched silicon sample

5 Effect of operating parameters on silicon levitation

5.1 Effect of specimen mass

Heating profiles of silicon-iron specimens containing 15 mass% iron, are shown in Figure 8. The levitation facility provides rapid heating and permits most specimens to reach a molten state in less than 100 seconds. Under a constant applied power and frequency, the droplet heating rate increases with increasing specimen mass, which adds to the absolute amount of iron in the silicon alloy specimen, resulting in additional heat gain through induction. Temperatures more than 200 K above the melting point can be achieved using heavier specimens.

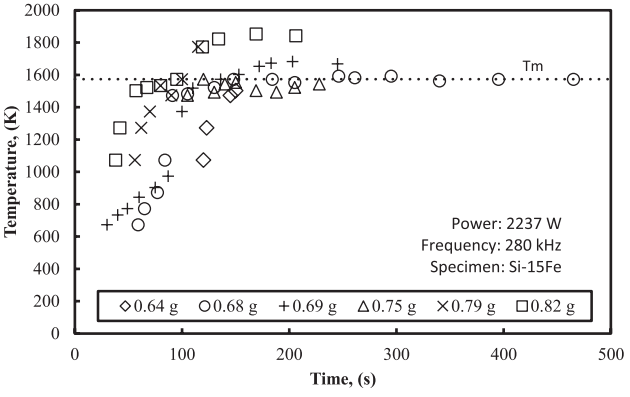

Fig. 8: Heating profiles for silicon-iron droplets containing 15% iron

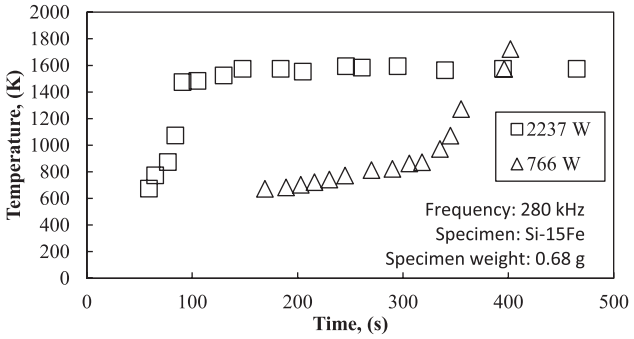

Fig. 9: Heating behavior of silicon-iron alloy droplets at two levels of applied power

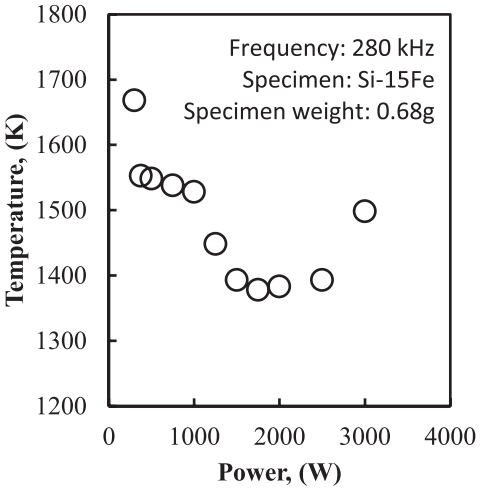

Fig. 10: Effect of applied power on the steady state temperature of silicon-iron alloy droplet

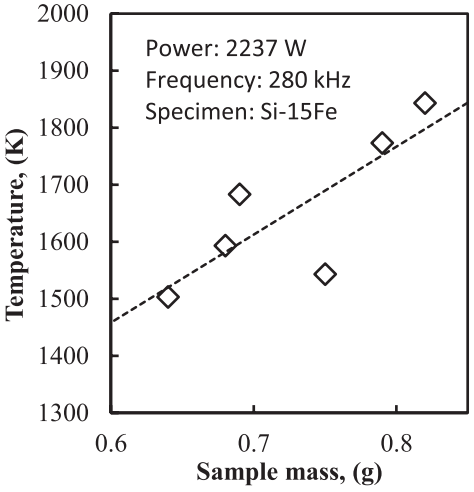

Fig. 11: Effect of specimen mass on droplet temperature

5.2 Effect of applied power

The magnitude of power applied to the coil controls the vertical position of the droplet within the electromagnetic field, which, in turn determines the density of electromagnetic field lines that interact with the droplet. The effect of applied power on droplet heating behavior is shown in Figure 9. The increase in heating rate at approximately 900 K is attributed to the silicon responding to the applied field and beginning to generate heat by induction.

By decreasing the power supplied to the coil, the lifting force is reduced and the droplet is located lower within the bottom coil, where the field flux is higher. As a result, the droplet temperature increases. Conversely, by increasing power to the coil, the droplet sits higher within the electromagnetic field where the flux is weaker and consequently lower temperatures are achieved. However, upon reaching a minimum temperature, further increase in applied power will lift the droplet higher into the electromagnetic field associated with the upper coil where the flux is greater and this will cause the droplet temperature to increase again, as shown in Figure 10. The effect of specimen mass on droplet temperature at fixed power input is shown in Figure 11. By controlling these parameters precise droplet temperatures within the desired range can be achieved.

6 Future work

An investigation is currently underway to study the thermodynamic behaviour of phosphorus dissolution in silicon and silicon-iron alloys using the levitation system described in this paper. Phosphorus partial pressure will be controlled by heating red phosphorus in a stream of purified argon which then transports the phosphorus vapor to the levitated metal droplet.

Factors affecting the removal of phosphorus from silicon and silicon-iron alloys will be examined by exposing the levitated droplets to controlled atmospheres under reduced pressure. These experiments are being conducted in order to provide a foundation of fundamental knowledge which could ultimately lead to the development of a new method for the mass production of solar grade silicon at a relatively low cost. The results of these studies will be reported in a subsequent publication.

7 Conclusions

1. Electromagnetic levitation of silicon was achieved using a pre-heating procedure by means of which solid silicon was heated by conduction while posi-

tioned on a high purity graphite disc which in turn was located within the electromagnetic field. With increasing temperature, the resistivity of the silicon is decreased and at approximately 1100 K the solid silicon responds to the applied field and begins to levitate.

2. Pre-heating is also necessary with silicon-iron alloys but this can be achieved without utilizing the graphite disc. Iron within the silicon alloy is responsible for providing induction heating to the entire specimen. At temperatures in the vicinity of 900 K, silicon-iron specimens respond to the applied field and begin to levitate.
3. With the aid of an appropriate coil design the effect of specimen weight and applied power on droplet temperature was investigated. Under a constant applied power and frequency, the droplet heating rate increases with increasing specimen mass. Reducing the lift force by decreasing the power will allow the droplet to position lower within the coil, where the field flux is stronger. As a result, the droplet temperature increases. Conversely, the droplet temperature is able to remain at the lower end of the temperature range if the droplet sits higher within the electromagnetic field. This is achieved by increasing power to the coil. However, upon reaching a minimum temperature, further increase in applied power will increase the droplet temperature due to positioning of the sample within the reversed turn region of the coil where the flux density again increases.
4. The rapid heating nature of electromagnetic levitation permits most silicon and silicon-iron specimens to reach the molten state in less than 100 seconds.

Appreciation is expressed to the Natural Sciences and Engineering Research Council of Canada who provided funding for this project through a Strategic Research Grant.

Received: October 3, 2013. Accepted: November 27, 2013.

References

[1] T. Ikeda and M. Maeda, *ISIJ Int.*, **32** (1992) 635–642.
[2] T. Yoshikawa and K. Morita, *Sci. Tech. Adv. Mater.*, **4** (2003) 531–537.
[3] K. Morita and T. Miki, *Intermetallic*, **11** (2003) 1111–1117.
[4] T. Miki, K. Morita and N. Sano, *Metall. Mater. Trans. B*, **27B** (1996) 937–941.
[5] S. Ueda, K. Morita and N. Sano, *Metall. Mater. Trans. B*, **28B** (1997) 1151–1155.
[6] K.X. Wei, W.H. Ma, Y.N. Dai, B. Yang, D.C. Liu and J.F. Wang, *Trans. Nonferrous Soc. China,* **17** (2007) 1022–1025.
[7] S. Asai, *Electromagnetic Processing of Materials*, Springer, Dordrecht, (2012), pp. 52–95.
[8] N. El-Kaddah and J. Szekely, *Metall. Mater. Trans. B*, **14B** (1983) 401–410.
[9] W.H. Hayt and J.A. Buck, *Engineering Electromagnetics*, McGraw Hill, New York, (2001), pp. 224–238.
[10] B. Harris and A.E. Jenkins, *J. Sci. Instrum.*, 36 (1959) 238–240.
[11] A. Kermanpur, M. Jafari and M. Vaghayenegar, *J. Mater. Proc. Tech.*, **211**(2) (2010) 222–229.
[12] K. Kuribayashi and T. Aoyama, *J. Cryst. Growth*, **237–239**, (3) (2002) 1840–1843.
[13] Z. Jian, K. Kuribayashi and W. Jie, *Mater. Sci. Forum*, **475–479** (2005) 2603–2606.
[14] Y. Inatomi, F. Onishi, K. Nagashio and K. Kuribayashi, *Int. J. Thermophys.*, **28**(1) (2007) 44–59.
[15] Y. Asakuma, S.H. Hahn, Y. Sakai, T. Tsukada, M. Hozawa, T. Matsumoto, H. Fujii, K. Nogi and N. Imaishi, *Metall. Mater. Trans. B*, **31B** (2000) 327–329.
[16] H. Fujii, T. Matsumoto, N. Hata, T. Nakano, M. Kohno and K. Nogi, *Metall. Mater. Trans. A*, **31A** (2000) 1585–1589.
[17] D.L. Li, X.M. Mao and H.Z. Fu, *J. Mater. Sci. Lett.*, **13** (1994) 1066–1068.
[18] M. Przyborowski, T. Hibiya, M. Eguchi and I. Egry, *J. Cryst. Growth*, **151** (1995) 60–65.
[19] D. Li and D.M. Herlach, *Europhys. Lett.*, **34**(6) (1996) 423–428.